GENERAL RESEARCH

Critical Gas Velocity for Suspension of Solid Particles in Three-Phase Bubble Columns

Mathew Abraham, Ashok S. Khare, Sudhirprakash B. Sawant,* and Jyeshtharaj B. Joshi
Department of Chemical Technology, University of Bombay, Matunga, Bombay 400019, India

The critical gas velocity for suspension of solid particles was studied in 200-mm- and 385-mm-i.d. bubble columns. The terminal settling velocity was varied in the range 8.2–290 mm/s, and the volume of solids per unit cross-sectional area of the column was varied from 5.8–80 mm (0.05–5% by volume). The effects of sparger design and the column height have been investigated. A rational correlation has been proposed.

Introduction

Three-phase bubble columns are widely used in industry for hydrogenation, oxidation, alkylation, chlorination, ammonolysis, conversion of synthesis gas into hydrocarbons, bacterial leaching processes, and biological wastewater treatment (Shah, 1979; Doraiswamy and Sharma, 1984; Joshi et al., 1985, 1988). In the three-phase bubble columns the gas phase provides energy for generating intense turbulent flow in the liquid phase. This liquid motion imparts energy to the solid phase by which they can remain in suspended condition. The solid phase acts as a catalyst, undergoes a chemical reaction, or may remain inert. For the effective utilization of three-phase bubble columns, the solid phase needs to remain in suspended condition. For this purpose, a minimum value of superficial gas velocity (V_{GC}) is needed. The knowledge of V_{GC} is crucial for the design of three-phase bubble columns. Investigations in this respect have been carried out by Roy et al. (1964), Imakufu et al. (1968), Narayanan et al. (1969), Koide et al. (1983, 1984, 1986), Pandit and Joshi (1984, 1987), Smith et al. (1986), and Heck and Onken (1987). Experimental conditions and the range of variables covered in these studies are summarized in Table I. Correlations proposed by these workers for V_{GC} are listed in Table II.

Literature Survey

Roy et al. (1964) have measured the critical solid holdup that can remain suspended at a given value of gas velocity. They studied the effect of sparger design, solid particle size, liquid surface tension, liquid viscosity, and solid–liquid wettability on critical solid holdup and proposed an empirical correlation in terms of dimensionless groups containing these parameters. They observed two regions of critical solid holdup with gas velocity. In the first region of lower gas velocity, the critical solid holdup depends on the nature of the sparger. In the second region of higher gas velocity, the critical solid holdup was found to be independent of the nature of the sparger. For quartz particles, the second region was found to exist for values of $V_G > 0.28$ m/s. However, these authors carried out their experiments with a relatively smaller column of 50.8-mm i.d. It is known that the flow pattern in large columns (>150-mm i.d.) is substantially different from the flow pattern in small columns.

Imakufu et al. (1968) studied the effect of solid concentration, sparger design, and the shape of the column bottom on V_{GC}. They used 50-, 100-, and 200-mm i.d. columns. They observed, contrary to the findings of Roy et al., that V_{GC} decreases with increasing solids concentration. They also reported that, in the 50-mm column, the sparger design had no effect on V_{GC}. They observed that V_{GC} increases with increasing column diameter. Further, they have pointed out that for larger diameter columns the shape of the column bottom and the position of the sparger had a strong influence on V_{GC}.

Narayanan et al. (1969) have studied the solid suspension in 114- and 141-mm-i.d. columns with a H_C/T ratio of 1. The particle size was varied in the range of 125–600 μm. The results are very useful. It was observed that V_{GC} increases with an increase in the column diameter. Empirical correlations have been suggested for predicting V_{GC}. However, the value of V_{GC} is known to depend on the H_C/T ratio, and the commonly used H_C/T ratio is greater than 4.

Koide et al. (1983) worked with 100-, 140-, and 300-mm-i.d. columns and a conical bottom section such that the ratio D_d/T could be varied. The particle size was varied so as to give a range of terminal settling velocity of 4–74.9 mm/s. They reported that V_{GC} increases with increasing particle size, solid loading, and column diameter. They reported no effect of liquid height on V_{GC} in the range of H_C of 0.50–1.50 m (H_C/T ratio of 3.33–10). They also observed that a reduction in V_{GC} can be achieved by using a conical bottom with a small value of D_d/T. However, the conical bottom was not so effective in the larger diameter column as compared to the smaller diameter column used. These authors also observed that the correlation of Roy et al. (1964) predicted very low values of V_{GC} as compared with their experimental values. This difference was attributed to the use of a small size column by Roy et al. (1964). Also they observed that the correlation of Narayanan et al. (1969) predicted higher values of V_{GC} when compared with their data which may be due to the fact that Narayanan et al. used a much smaller value of H_C/T of 1 as compared to that used by Koide et al.

Pandit and Joshi (1984) carried out a systematic work on V_{GC} with an air–water system and for a wide range of

*To whom correspondence should be addressed.

0888-5885/92/2631-1136$03.00/0

particle sizes (110–2000 μm). They have also presented the effect of ϵ_S, the H_C/T ratio and column diameter on V_{GC}. They observed for the first time that the dependence of V_{GC} on the particle size and density (both represented by the particle settling velocity, $V_{SN\infty}$) depends upon the range of $V_{SN\infty}$. Further, when the V_{GC} values are quite high (i.e., for particles with $V_{SN\infty} > 100$ mm/s), they recommended the use of continuous liquid so as to reduce V_{GC}.

Koide et al. (1984) have reported the values of V_{GC} of bubble columns with and without draught tubes and have observed that the introduction of draft tube reduces the value of V_{GC}.

Koide et al. (1986) have systematically studied the effects of column dimensions, properties of the solid particles, and mixed particle sizes on V_{GC} in bubble columns with and without a draft tube. It was observed that the effect of column dimensions on V_{GC} of mixed solid particles was similar to those on V_{GC} of monosize particles. V_{GC} decreased with decreasing weight fraction of the solid particles having the largest value of $V_{SN\infty}$ among the solid particles used, and the properties of solid particles other than the largest particles had almost no effect on V_{GC}. On the basis of these observations, they proposed a method to estimate V_{GC} for particle mixtures using the correlation of Koide et al. (1983) for monosize particles.

Smith et al. (1986) modified the sedimentation dispersion model for describing the axial concentration distribution of solids in slurry bubble columns. Using this model a criterion for complete and incomplete suspension of particles was developed. This model gives very conservative estimates of V_{GC}.

Heck and Onken (1987) reported a hysteresis effect in the measurements of V_{GC}, in bubble columns with and without a draft tube. They reported that the minimum gas velocity for maintaining the solids in suspension when the superficial gas velocity was increased from zero was higher than when the gas velocity was reduced from a high value.

Pandit and Joshi (1987) reported the effects of surface tension, liquid viscosity, pseudoplasticity, drag reducing agents, and the prescence of electrolytes on V_{GC} in a 200-mm-i.d. column. They have proposed a mathematical model for the prediction of V_{GC} in batch and continuous modes of the liquid phase.

A careful analysis of the foregoing published literature reveals the following points. (1) The effect of gas sparger design on V_{GC} needs to be investigated in detail. The effects of hole size, number of holes, and free area need systematic attention. (2) A systematic set of experiments are needed to understand the effect of the height to diameter ratio on V_{GC}. The present work is concerned with these two aspects. Further, a generalized correlation has also been developed.

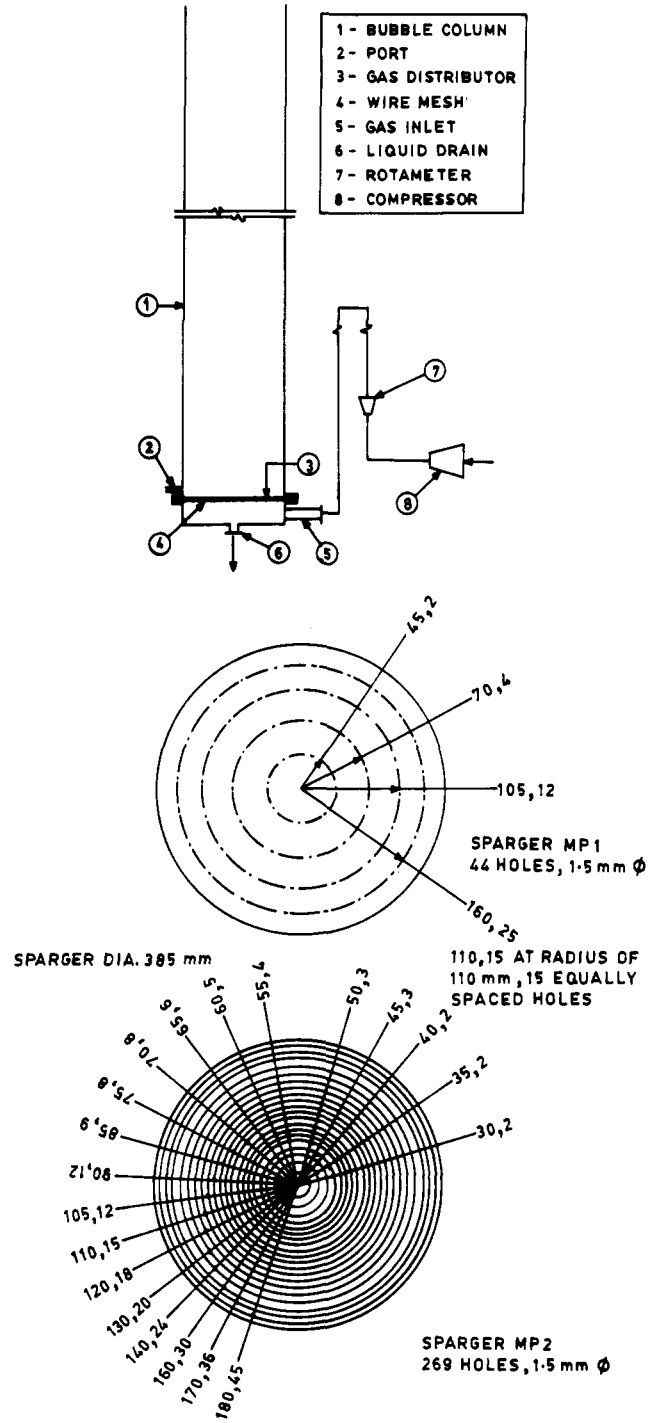

Figure 1. (a, top) Experimental setup. (b, bottom) Details of sparger design.

Experimental Section

Experiments were carried out in 200- and 385-mm-i.d. bubble columns. Air and water formed the gas and liquid phases, respectively. The solid phase consisted of alumina particles and spherical glass beads. The particle size was varied in the range of 60–2100 μm, and the volume of solids per unit cross-sectional area of column was varied from 5.8 to 80 mm. The details pertaining to the solid phase are given in Table III. The terminal settling velocities of the solid particles were experimentally determined from measurements of settling velocities of particles in a 0.070-m-i.d. column. Also shown in Table III are values of terminal settling velocity obtained by calculation from a balance of forces (Perry and Chilton, 1984). To study the effect of sparger design, five spargers were used in the 385-mm column and two spargers were used in the 200-mm column. Both single orifice and multiorifice spargers were studied. The multiorifice spargers were essentially sieve plates with uniformly distributed orifices of 1.5-mm diameter. The number of holes was varied. In order to prevent the weeping of solid particles, the sieve plate was covered with a wire mesh. The details of the spargers and the wire mesh used in the two columns are given in Tables IV and V. A typical experimental setup is shown in Figure 1a. Figure 1b shows details of spargers MP1 and MP2 in the 385-mm column. Spargers MP3, MP4, and MP5 had orifices on a triangular pitch.

The column was operated in a semibatch manner with known volumes of liquid and solid forming the batch through which air was continuously sparged. The effect

Table I. Summary of Previous Work on Critical Gas Velocity for Suspension of Solid Particles in Bubble Columns

no.	investigator	T/m	column height/m	sparger design	system	d_p/μm
1	Roy et al. (1964)	0.05	1.5	sieve plate; effect of sparger design studied; four orifice plates employed with 4, 7, 13, and 19 holes with diff diams and at various posns	(liquid) H_2O, H_2O + alcohol (up to 28% (w/w)), til oil, compressor oil; (gas) air, N_2; (solid) quartz, Ni-Al alloy, coal, F-T catalyst	quartz: 130, 210, 346, 395, 675 coal: 603 Ni-Al alloy: 127 F-T catalyst: 348
2	Narayanan et al. (1969)	0.114 0.141	0.114 0.141	sieve plate with hole size of 0.159-cm diam and 120 and 156 holes	air-H_2O-quartz	quartz: 125, 210, 395, 675
3	Koide et al. (1983)	0.1 0.14 0.3	2.0 2.0 1.9	perforated plate covered with 260-300 mesh stainless steel wire gauze; gas distributor diam varied using a conical bottom	(liquid) demineralized H_2O, glycerol aq soln (44 and 77% (w/w)), ethylene glycol aq soln (70% (w/w)); (solid) glass, bronze; (gas) air	glass: 77, 89, 147, 198, 501, 846 bronze sphere: 167
4	Imakufu et al. (1968)	0.05, 0.1, and 0.2	1.0 2.0	(a) porous plate made by sintering 10-μm-size stainless steel particles; (b) perforated plates with 1, 3, and 13 holes (hole diam = 0.2 cm) in 0.10-m column; (c) conical bottom in 0.20-m column	air-H_2O-glass	glass: 111
5	Pandit and Joshi (1984)	0.1, 0.2 0.385		perforated plate (sieve plate; 180 equally spaced, 2-mm-diam holes)	air-H_2O-quartz/glass particles; effect of V_L also studied	70 110 210 340 500 850 2000
6	Pandit and Joshi (1987)	0.2	2.45	perforated plate (180 equally spaced 2-mm-diam holes)	air-quartz/glass; (liquids) electrolyte aq soln (NaCl, KCl), methanol, ethanol, butanol aq soln (surface tension = 61-72 mN/m), glycerine, guar gum (0.125, 0.25, 0.5% (w/w)), CMC (0.25, 0.5, and 1% (w/w); viscosity 1-30 mPa·s), drag reducing agent (PAA) (500, 1500 ppm)	110 340 500 850 2000
7	Heck and Onken (1987)	0.2	2.5	perforated plate fixed in the conical bottom (cone angle of 60°) with plate diam of 0.08 m and holes of 0.8 mm (free cross-sectional area = 0.54%)	air-H_2O-glass spheres; with and without draft tube (DT)	308
8	Smith et al. (1986)	0.0762	1.54	sieve plate glass distributor with 31 holes of 1-mm diam	air-H_2O-glass beads or carborundum	glass: 48.5, 81 carborundum: 84
9	Koide et al. (1984)	0.1, 0.14 0.218, 0.3	2.3	perforated plate covered with stainless steel, 260-300-mesh wire gauze; conical bottom with cone angle of $\pi/3$ rad; variation of diam of gas distributor, no. of holes, and hole diam	air-H_2O, glycerol and glycol aq solns; with and without draft tube	glass spheres: 117 136 198 498 high index glass spheres: 79 bronze sphere: 89
10	Koide et al. (1986)	0.14 Di = 0.066 Di = 0.082 Di = 0.094 Di = 0.104	2.30	conical bottom with $\pi/3$ rad cone angle, perforated plate covered with 260-300 mesh stainless steel wire gauze; gas distributor diam (0.035-0.14 m) varied along with hole diam (1-3 mm) and no. of holes (3-7 with DT and 55 without DT)	air-H_2O-glass spheres	glass spheres: 79 106 200 high index glass sphere: 79

of static slurry height was studied by varying the clear liquid height (H_C) to diameter (T) ratio from 0.5 to 7 in the 385-mm column. In the 200-mm column, the H_C/T ratio was kept at 8. Fractional gas holdup was measured by noting the difference between the dispersed and clear liquid heights. Roy et al. (1964) have described three methods for the measurement of V_{GC}, namely, from visual observations, pressure drop measurements, and a sampling technique. However, visual observations are most commonly used and were also used in this work. A known quantity of solid particles was settled in the liquid at a particular value of the height of slurry. From behind the column a strong narrow beam of light was focused on the gas sparger. When the gas velocity was low, most of the particles rested on the sparger. As the gas velocity was slowly increased, more and more of particles on the sparger became suspended. The value of V_G at which particles or particle aggregates did not remain on any part of the bottom of the column for more than 1-2 s was noted as V_{GC}. In order to check the possibility of hysteresis, a high value of V_G ($\gg V_{GC}$) was selected, where all the particles were suspended. Then V_G was continuously reduced to get V_{GC}. However, it was observed that the value of V_{GC} obtained by these two methods agreed within 5%, and we did not observe hysteresis. For all the measurements of V_{GC}, this procedure was repeated, and the value of V_{GC} reported is the average of the two values of V_{GC} obtained. Also for any particle size and sparger design, the maximum value of solid loading was chosen such that V_{GC} did not exceed 0.30 m/s. Values of V_{GC} beyond this are unlikely to be encountered in the commercial practice.

Results and Discussion

Effect of Terminal Settling Velocity of Particle, $V_{SN\infty}$. Figure 2a shows the effect of $V_{SN\infty}$ on V_{GC} in the 385-mm column at $H_C/T = 4$ with two spargers MP2 and

ρ_S/(kg/m^3)	$V_{SN\infty}$/(m/s)	solid loading or solid concn	V_G/(m/s)	V_L/(m/s)	measurement technique and remarks
2630	0.0135–0.11 (air–H_2O–quartz)	7–15% (w/w)			expts performed for the critical solid holdup, defined as the point where all the solid particles were just brought into suspension; (1) visual, (2) pressure drop, and (3) sampling methods; batch mode; correlation proposed
1440					
3466					
2601					
2630	0.0125–0.11	2.5–18% (w/w)	0.05–0.23		visual observation method; batch mode; correlation presented
2500	0.0048–0.0749	0–400 kg/m^3 of slurry	0.015–0.2		(1) visual and (2) pressure drop methods; batch mode; study aimed at clarifying the effects of column diam, properties of liquid and solid particles, and shape of column bottom on V_{GC}; correlation proposed
8770	0.0671				
2550	0.0103	15.6–81.3 kg of solid/(m^3 of slurry)	0.03–0.2		pressure drop measurement method; hysteresis observed if V_G increased and then decreased; results reproducible when V_G decreased gradually; batch mode; position of liquid inlet also important if in continuous mode
2260	0.0085	0–10% (v/v)	0–0.80	0–0.08	visual method; batch mode; effects of d_p, H_C/T ratio, and column diam studied; mathematical model based on V_C and U' was proposed
2260	0.0125				
2500	0.05				
2500	0.076				
2500	0.104				
2500	0.134				
2500	0.164				
2260	0.0125	0–10% (v/v)	0–0.06		visual method; batch mode; study aimed at rationalizing the variation in the superficial gas velocity for suspension in TPSR on the basis of variation in the liquid-phase physical properties; quantitative correlations and predictive methods proposed for predicting V_{GC}
2500	0.076				
2500	0.104				
2500	0.134				
2500	0.164				
2440		2–20% (v/v)	0–0.2		pressure drop method near the gas distributor plate; batch mode; study aimed at showing the occurrence of pronounced hysteresis effect in solid suspended bubble column with and without draft tube
2420	0.0020–0.0070	up to 10% (w/w)	0.031–0.20		(1) visual method and (2) method of measurement of solids concn at the bottom of the column as a function of V_G (at V_{GC}, discontinuity in this relation occurs); study aimed at using the modified sedimentation dispersion model for developing a criterion to predict V_{GC}
3870	0.021				
		25–400 kg of solid/(m^3 of slurry)	0–0.1		visual and pressure drop methods; batch mode; study aimed at experimentally determining the effects of column dimensions and properties of the liquid and solid particles on V_{GC} with draft tube; effect of $V_{SN\infty}$, C_S, and height of draft tube studied; correlation proposed; V_{GC}, with conical bottom and draft tube, (1) increased with increase in $V_{SN\infty}$, C_S, diam of gas distributor, and ρ_S and decreased with increase in T and μ_L and (2) decreased with introduction of draft tube
2500	0.0109				
2500	0.014				
2500	0.0244				
2500	0.0779				
4680	0.0125				
8770	0.0291				
		av concn: 100 kg of solid/(m^3 of slurry) (however in a mixture, wt fracn of largest particles varied in range of 0–1)	0–0.022		visual and pressure drop methods; batch mode (with and without draft tube); study aimed at experimentally clarifying the effects of column dimensions, properties of solid particles, and composition of solid mixtures on V_{GC} (multicomponent solid system); correlation proposed
2500					
2500					
2500					
4680					

MP3. Figure 2b shows the effect of $V_{SN\infty}$ on V_{GC} in the 200-mm column at $H_C/T = 8$ with two spargers MP4 and MP5. From these figures it is seen that two distinct regimes prevail, for both columns used. For particles with $V_{SN\infty}$ up to 100 mm/s, V_{GC} is approximately proportional to $V_{SN\infty}^{0.45}$. For particles above this size range, V_{GC} was found to vary as $V_{SN\infty}^{0.89}$. Koide et al. (1983) have reported that $V_{GC} \propto V_{SN\infty}^{0.76}$ for $V_{SN\infty}$ in the range of 4–75 mm/s.

Effect of Volume of Solids per Unit Cross-Sectional Area, ϵ'_S. Figure 2c shows the effect of ϵ'_S on V_{GC} in the 385-mm column at $H_C/T = 4$ with two spargers MP2 and MP3. Figure 2d shows the effect of ϵ'_S on V_{GC} in the 200-mm column at $H_C/T = 8$ with two spargers MP4 and MP5. For particles of size less than 600 μm (corresponding to $V_{SN\infty}$ less than 100 mm/s), V_{GC} was found to vary as $\epsilon'_S{}^{0.25}$ in both columns. For particles of size equal to or greater than 600 μm, V_{GC} was found to vary as $\epsilon'_S{}^{0.57-0.78}$. Pandit and Joshi (1984) also reported V_{GC} to vary as $\epsilon'_S{}^{0.2-0.3}$ for smaller size particles (<100 μm). Koide et al. (1983) have reported V_{GC} to vary as $\epsilon'_S{}^{0.14}$ for particles having $V_{SN\infty}$ between 4 and 75 mm/s.

Effects of Sparger Design and Height to Diameter Ratio. Figure 2a shows a comparison between the values of V_{GC} obtained in the 385-mm column with spargers MP2 and MP3. It can be seen that sparger MP2 which had a lower percent free area (0.42%) as compared to MP3 (8.6%) gave higher values of V_{GC}. Figure 3 is a comparison of the solid loadings that could be suspended by different gas spargers in the 385-mm column at a value of V_G between 0.15 and 0.17 m/s. It is seen that, at this velocity, sparger MP2 (% free area = 0.42) could suspend 250-μm particles up to ϵ'_S = 23.4 mm, sparger MP1 (% free area = 0.067) up to 1.17 mm, sparger SP2 up to 0.12 mm, and sparger SP1 up to 0.02 mm. It can be seen that the single point spargers are very inefficient. For these spargers the liquid circulation is very weak in certain regions of the

Table II. Correlations Proposed for V_{GC}

no.	investigator	correlations proposed
1	Roy et al. (1964)	$C'_S = 6.84 \times 10^{-4}[Re_T^{1.0} N_B^{-0.23}(V_t/V_b)^{-0.18}(\nu')^{-3.0} C_\mu]$ for $Re_T < 500$ $C'_S = 0.1072[Re_T^{0.2} N_B^{-0.29}(V_t/V_b)^{-0.18}(\nu')^{-3.0} C_\mu]$ for $Re_T > 600$
2	Narayanan et al. (1969)	$V_{ZB} = V_{GT} + 0.03687\,(V_G H_{SL})^{1/2}$ $V_G < 0.067$ m/s $V_{ZB} = V_{GT} + 0.05378(V_G^{0.38} H_{SL})^{1/2}$ $0.067 < V_G < 0.21$ m/s $V_S = \left(2 \times 10^{-4} g(\rho_S - \rho_L)\left[\frac{2d_p}{3\rho_L} + \frac{H_S H_{SL}}{\rho_S + H_S \rho_L}\right]\right)^{1/2}$ when $V_{ZB} = V_S$ = particle is suspended $V_{GE} = 4.30[50T]^n e^{-0.1B} V_{GT}$ $B < 10$ $V_{GE} = 1.25[50T]^n e^{-0.03B} V_{GT}$ $B > 10$ for $d_p > 200$ μm, $n = 0.5$ $d_p < 100$ μm, $n = 0.2$
3	Koide et al. (1983)	$\frac{V_{GC}}{V_{SN\infty}} = 0.801\left(\frac{\rho_S - \rho_L}{\rho_L}\right)^{0.6}\left(\frac{C_S}{\rho_S}\right)^{0.146}\left(\frac{(gT)^{1/2}}{V_{SN\infty}}\right)^{0.2}\left\{1 + 807\left(\frac{g\mu^4}{\rho_L \sigma^3}\right)^{0.578}\right\}\left(1 - 1.2(1 - D_d/T)^{0.0301(T^2 g\rho_L/\sigma)^{0.559}}\right)$
4	Pandit and Joshi (1984, 1987)	*Homogeneous Regime*: The particle gets suspended when the average liquid velocity in the vicinity of solid particle (V_C) is equal to $V_{SN\infty}$. The value of V_C is given by $V_C = \left(\frac{\delta\epsilon_G}{1 - \epsilon_G - \delta\epsilon_G - \bar{\epsilon}_S}\right) V_{b\infty}$ *Heterogeneous Regime*: In this regime particles get suspended when the value of $U' \approx V_{SN\infty}$. U' is given by $U' = 0.3275\left\{\frac{gT}{\rho_C - \rho_G}[(V_G + V_L)(\rho_C - \rho_G)(1 - \epsilon_G) - (\rho_C - \rho_G)\epsilon_G V_{b\infty} - \bar{\epsilon}_S V_{SN}(\rho_S - \rho_C) - V_L \rho_L]\right\}^{1/3}$ where $\rho_C = \bar{\epsilon}_S \rho_S + \epsilon_L \rho_L$ and for batch mode $V_L = 0$.
5	Koide et al. (1984, 1986)	$\frac{V_{GC}}{V_{SN\infty}} = 4.60\left(\frac{C_S}{\rho_S}\right)^{0.273}\left(\frac{\rho_S - \rho_L}{\rho_L}\right)^{0.75}\left(\frac{V_{SN\infty}\mu}{\sigma}\right)^{-0.634}\left(\frac{T^2 g\rho_L}{\sigma}\right)^{-0.34}\left(\frac{S_o}{S_\alpha}\right)^{0.546}\left(\frac{S_o}{S_i}\right)^{0.454} \times$ $\left\{1 + 897\left(\frac{g\mu^4}{\rho_L\sigma^3}\right)^{0.29}\right\}\left\{\left(\frac{V_{SN\infty}}{(gH)^{1/2}}\right) + 1.47 \times 10^{-4}\left(\frac{H}{T}\right)\right\}\left(1 - 1.32(1 - D_d/T)^{0.99(T^2 g\rho_L/\sigma)^{0.173}}\right)$ $8.55 \le (C/\rho_S) \le 0.16$ $1.12 \le (\rho_S - \rho_L/\rho_L) \le 7.80$ $1.31 \times 10^{-4} \le \left(\frac{V_{SN\infty}\mu}{\sigma}\right) \le 9.67 \times 10^{-4}$ $1.36 \times 10^{3} \le \left(\frac{T^2 g\rho_L}{\sigma}\right) \le 1.22 \times 10^{4}$ $1.68 \times 10^{-11} \le \left(\frac{g\mu^4}{\rho\sigma^3}\right) \le 1.62 \times 10^{-6}$ $0.18 \le (D_d/T) \le 0.5$ $5 \times 10^{-4} \le \left(\frac{V_{SN\infty}}{(gH)^{1/2}}\right) \le 2.10 \times 10^{-2}$ $4.67 \le (H/T) \le 15$ $0.22 \le (S_i/S_o) \le 0.552$
6	Smith et al. (1986)	For complete suspension of solid particles the following equation must be satisfied: $\bar{C}_S < \frac{(0.155 \ln d_p + 1.78)\rho_S(\exp(A) - 1)}{(1 - \epsilon_G)(1 - A)A}$ where $A = -(\epsilon_L V_{SN} H_D/D_S)$.

bottom section (up to a height equal to the column diameter) and the dead zone in this region (where there are no gas bubbles) is quite large. The presence of such large dead zones above the sparger plates with single orifices explains the poor efficiency of these spargers. In the case of multipoint spargers, the V_{GC} was found to decrease with an increase in the number of holes due to the reduction of stagnant dead zones. For instance, an increase in the number of holes from 44 to 269 in the 385-mm-i.d. column decreases V_{GC} by a factor of 3. However an increase from 269 to 5684 decreases V_{GC} by only 15%.

In order to study the effect of a very large number of sparger holes, experiments were conducted in the 200-mm-i.d. column with wire mesh placed above the sieve plate, resulting in sparger MP5. When the wire mesh was placed below the sieve plate (sparger MP4), a finite number of sparging points (180 points) was obtained. The values of V_{GC} obtained with these two spargers is compared

Table III. Details of Particles Used in the Present Investigation

setup no.	av $d_p/\mu m$	$\rho_S/(kg/m^3)$	terminal settling velocity/(mm/s) exptl	theoret
1	67	4000	8	7
2	98	4000	16	15
3	150	2500	17	16
4	250	2500	36	33
5	450	2500	78	69
6	600	2500	108	94
7	900	2500	137	133
8	1200	2500	181	173
9	2100	2500	290	278

in Figure 2b. It is seen that sparger MP4 always gave a lower value of V_{GC} as compared to sparger MP5. When the wire gauze is above the sieve plate (as in sparger MP5), the resulting open area for the gas sparging is nothing but the open area of wire gauze (34%). However, when the wire gauze was placed below the sieve plate, the resultant open area of gas sparging is the area of 180 holes of the sieve plate, each of 1.5-mm size (1.0%).

Therefore at any gas flow rate, the orifice gas velocity will be much higher for sparger MP4 as compared to sparger MP5. Higher gas velocity at the sparger increases the local liquid circulation velocity which helps the solid suspension at lower gas velocity for sparger MP4 as compared to sparger MP5. Hence as the number of sparging points is increased indefinitely the reduction in V_{GC} due to reduction in stagnant dead zones is offset by the reduction in the hole velocity and results in an increase in V_{GC}.

From the foregoing discussion the following points may be emphasized: (i) Single point spargers are inefficient and should not be used; (ii) an increase in number from 1 to 44 and 1 to 269 decreases V_{GC} by a factor of 5 and 15, respectively. However a further increase in number decreases V_{GC} marginally (within 15%). Therefore, spargers MP2, MP3, MP4, and MP5 can be considered together for developing a correlation.

The effect of liquid height on V_{GC} for a given amount of solids was studied by varying the H_C/T ratio from 0.5 to 7 in the 385-mm column with sparger MP2 (Figure 4a–c). Figure 4a shows the effect of variation of the H_C/T ratio on V_{GC} with ϵ'_S as a parameter for 250-μm particles. Figure 4b shows the effect of H_C/T on V_{GC} for 600- and 900-μm particles and Figure 4c for 1200- and 2100-μm particles. Figure 4d shows the effect of H_C/T on V_{GC} with sparger MP1 for 250- and 600-μm particles. From these figures it is clear that above $H_C/T = 3$, the height of the slurry had no effect on values of V_{GC}. But below $H_C/T = 3$, V_{GC} increases as H_C/T decreases for a particular value of ϵ'_S. This observation indicates that the flow pattern in the sparger region is different from the bulk of the column.

In general a bubble column can be conveniently divided into two regions: (i) sparger region and (ii) bulk region. In the sparger region, the bubble size and the liquid-phase flow pattern are governed by sparger design. In the bulk region, the bubble size and the liquid-phase flow pattern are independent of the sparger design. The height of the sparger region depends upon the sparger design, V_G, and the liquid-phase physical properties. For a single point sparger, the height of the sparger region is large and it decreases with an increase in the uniformity of sparging. Joshi and Sharma (1979) and Joshi (1980) have analyzed the flow patterns, and the same are shown in Figure 5. Ueyama and Myauchi (1979) and Myauchi and Shyu (1970) have also described a model of the flow patterns in bubble columns in the bulk region. However to distinguish the sparger region and the bulk region, the model of Joshi (1980) has been chosen. The average liquid circulation velocity in the sparger region is given by Joshi and Sharma (1979) as

$$V_C = 1.31[gH_D(V_G - \epsilon_G V_{b\infty})]^{1/3} \quad (1)$$

whereas, in the bulk region, it is given by Joshi (1980) as

$$V_C = 1.31[gT(V_G - \epsilon_G V_{b\infty})]^{1/3} \quad (2)$$

Therefore, when the H_C/T ratio is large, the sparger region is negligible and the liquid circulation velocity is independent of the height of the sparger region, and V_{GC} also becomes independent of column height. When H_C/T is small (<3), most of the column volume is occupied by the sparger region. According to eq 1, the average liquid circulation velocity increases with column height and results in a decrease in the value of V_{GC}.

The effect of liquid height obviously depends upon the sparger design. For instance in the case of a single point sparger, the liquid height had influence on V_{GC} up to a high value of H_C as compared to that in multipoint spargers, as seen from Figure 3.

Review of the previous work reveals that the role of the sparger design on V_{GC} has not been successfully understood, and, hence, the variation in V_{GC} was explained on the basis of the overall behavior of the bulk region (characterized by the ϵ_G value). For example, Pandit and Joshi (1984) have mentioned that an increase in ϵ_G increases V_{GC}. Their observations are limited to a single sparger which does not show the effect of sparger design. The present work, however, clearly points out that not the bulk region but the sparger region dictates the variation of V_{GC}. Due to this, even though the ϵ_G is more for sparger MP4 as compared to sparger MP5, V_{GC} are lower for sparger MP4 than those observed with sparger MP5. Also the ϵ_G values in sparger MP1 and MP2 are similar; however, V_{GC} is much lower for sparger MP2 as compared to that for sparger MP1.

Hence results of the present investigation can be explained on the basis of sparger region. Solids are held in

Table IV. Details of Spargers Used

setup no.	column diam/mm	sparger	d_o/mm	no. of orifices	% free area	wire mesh	description
1	385	MP1	1.5	44	0.067	WM1	wire mesh below the sieve plate
2	-do-	MP2	-do-	269	0.42	-do-	-do-
3	-do-	MP3	-do-	5684	8.6	WM2	-do-
4	-do-	SP1	10	1	0.067	WM1	-do-
5	-do-	SP2	25	1	0.42	-do-	-do-
6	200	MP4	1.5	180	1.0	WM2	-do-
7	-do-	MP5	-do-	-do-	-34-	-do-	wire mesh above the sieve plate

Table V. Details of Wire Mesh Used

setup no.	wire mesh	mesh	gauge	wire diam/mm	aperture/mm	screening area/%
1	WM1	80	40	0.12	0.196	38
2	WM2	150	45	0.0711	0.0997	34

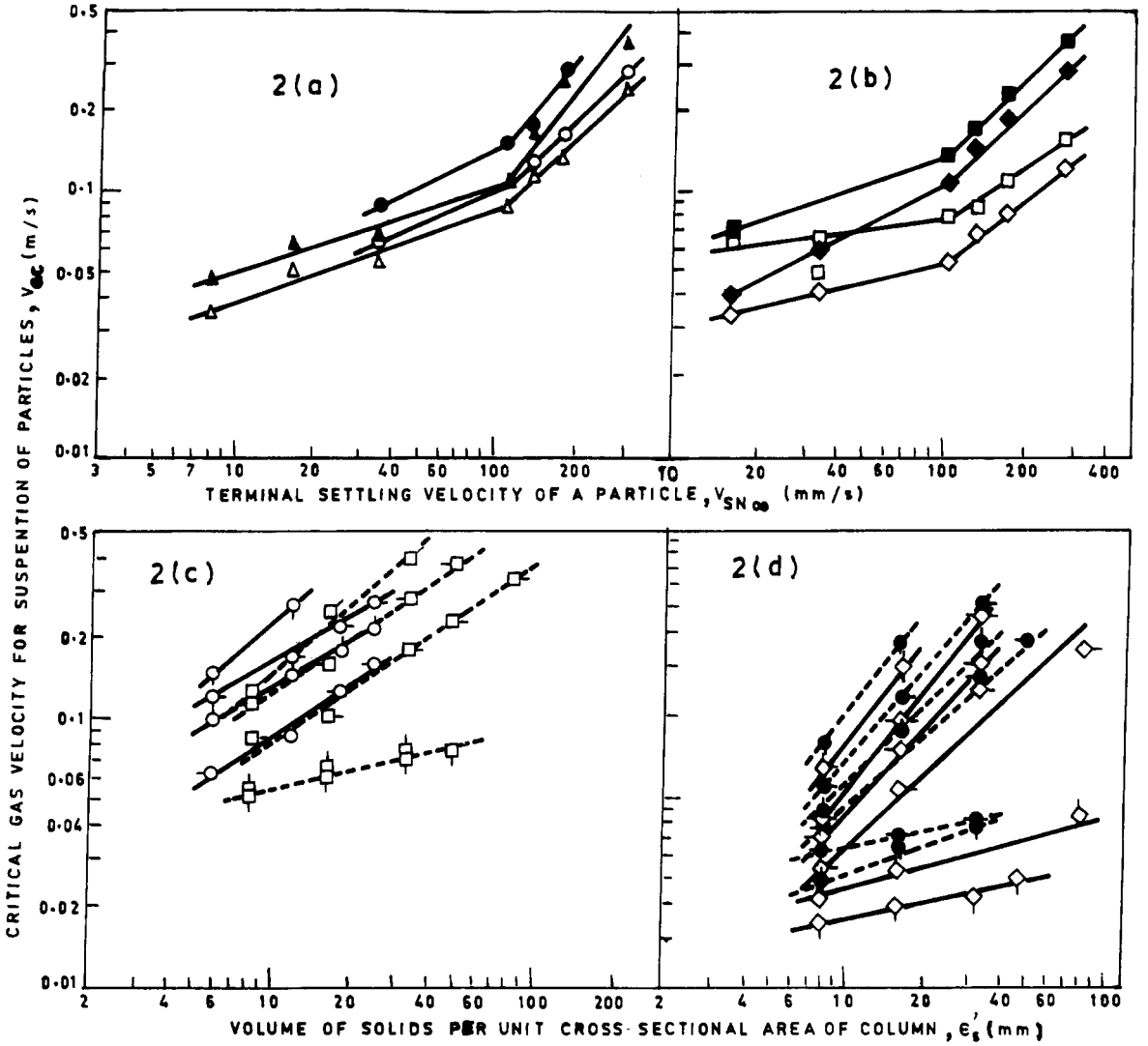

Figure 2. Effect of $V_{SN\infty}$ and ϵ'_S on V_{GC}. (a) For T = 385 mm, H_C/T = 4: (○) sparger = MP2, ϵ'_S = 5.8 mm; (●) sparger = MP2, ϵ'_S = 11.7 mm; (△) sparger = MP3, ϵ'_S = 8.0 mm; (▲) sparger = MP3, ϵ'_S = 16.0 mm. (b) For T = 200 mm, H_C/T = 8: (◇) sparger = MP4, ϵ'_S = 8.0 mm; (◆) sparger = MP4, ϵ'_S = 16.0 mm; (□) sparger = MP5, ϵ'_S = 8.0 mm; (■) sparger = MP5, ϵ'_S = 16.0 mm. (c) For T = 385 mm, H_C/T = 4: (-○) sparger = MP2, d_p = 250 μm; (◇) sparger = MP2, d_p = 600 μm; (○-) sparger = MP2, d_p = 900 μm; (◯) sparger = MP2, d_p = 1200 μm; (▯) sparger = MP3, d_p = 100 μm; (▯) sparger = MP3, d_p = 250 μm; (□-) sparger = MP3, d_p = 600 μm; (-□) sparger = MP3, d_p = 900 μm; (□) sparger = MP3, d_p = 1200 μm. (d) For T = 200 mm, H_C/T = 8: (◊) sparger = MP4, d_p = 100 μm, (◇) sparger = MP4, d_p = 250 μm, (◇-) sparger = MP4, d_p = 600 μm, (-◇) sparger = MP4, d_p = 900 μm, (-◇-) sparger = MP4, d_p = 1200 μm, (◊) sparger = MP4, d_p = 2100 μm, (◆) sparger = MP5, d_p = 100 μm, (-●-) sparger = MP5, d_p = 250 μm, (-●) sparger = MP5, d_p = 600 μm, (●) sparger = MP5, d_p = 900 μm, (●-) sparger = MP5, d_p = 1200 μm, (◆) sparger = MP5, d_p = 2100 μm.

suspension by the transfer of momentum from the gas phase to the solid phase via the liquid medium. Introduction of gas initiates liquid circulation, which will be responsible for the suspension of solids. A proper design of the gas sparger (hole size, number of holes, and open area for sparging) through which gas is sparged into the column (in the liquid medium) is thus necessary to take care of the initiation of liquid circulation required for solid suspension.

Effect of Column Diameter on V_{GC}. As seen from the previous discussion, V_{GC} depends on the volume of solids per unit cross sectional area (ϵ'_S) and the free cross-sectional area of sparger. Hence in a study of the effect of column diameter on V_{GC}, comparable values of ϵ'_S and free cross-sectional area of sparger need to be used in the two columns. Experiments were performed in the 200- and 385-mm-i.d. columns. Figure 6 shows the effect of column diameter on V_{GC}. Sparger MP2 having a free cross-sectional area of 0.42% was used in the 385-mm column, and sparger MP4 having a free cross-sectional area of 1.0% was used in the 200-mm column. From Figure 6 it is seen that V_{GC} is always higher in the 385-mm column within the range of particle sizes and solid loadings used in this work. The critical gas velocity for suspension of particles was found to vary as 0.27th power of column diameter.

However, using different spargers (different cross-sectional areas) in the two columns gives quite different results. Figure 7 shows the effect of column diameter on V_{GC} using sparger MP3 having 8.6% free cross-sectional area in the 385-mm column and sparger MP4 having 1% free cross-sectional area in the 200-mm column. From this figure it is seen that for 100-μm particles, V_{GC} is lower in the 200-mm column. In general, up to ϵ'_S = 16 mm and for any particle size (100–2100 μm), V_{GC} values in the 200-mm column were lower or equal to that in the 385-mm column. However for higher values of ϵ'_S (ϵ'_S > 32 mm), the trend is opposite and V_{GC} values in the 385-mm column were lower than those observed in the 200-mm column. Figure 8 shows the effect of column diameter on V_{GC} with sparger MP3 in the 385-mm column and sparger MP5 in the 200-mm column. It can be seen from this figure that

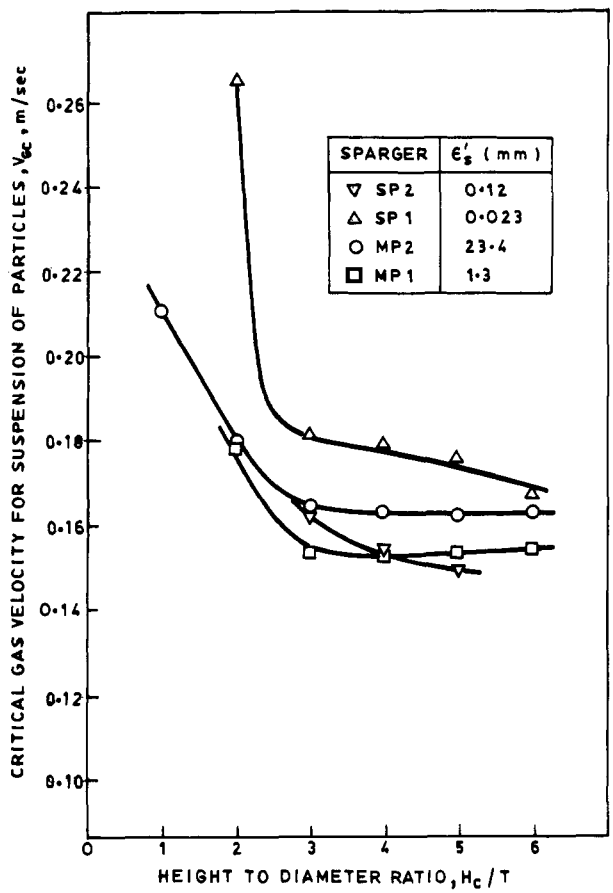

Figure 3. Comparison of the performance of different spargers in the 385-mm column.

the V_{GC} values observed in the 385-mm column are always lower than those in the 200-mm column.

Imakufu et al. (1968), Narayanan et al. (1969), and Koide et al. (1983) have observed that V_{GC} values increase with an increase in column diameter. Narayanan et al. observed that, for particles above 200 μm, $V_{GC} \propto T^{0.5}$ and, for particles below 100 μm, $V_{GC} \propto T^{0.2}$, for a fractional solid loading of 1–7% (v/v). Koide et al. (1983) observed that, for particles between 147 and 500 μm, $V_{GC} \propto T^{0.1}$ for a fractional solid loading between 1 and 4% (v/v). The higher exponent on T observed by Narayanan et al. (1969) may be partly due to the higher value of ϵ'_S in the larger diameter column as compared to that of the smaller diameter column.

Hence using spargers with similar open areas (MP2 and MP4) in the two columns, the V_{GC} values were always high in the larger diameter column. The increase in V_{GC} with an increase in column diameter may be due to the increase in the stagnant dead zones as T increases. However when spargers with different open areas are used in the two columns, the open area of the sparger and the column diameter affect V_{GC}. In Figure 7 the increase in V_{GC} due to an increase in the column diameter is offset by the decrease in V_{GC} with an increase in open area of sparging (MP3) in the larger column. In Figure 8, the decrease in V_{GC} with a decrease in the column diameter is offset by an increase in V_{GC} with a very large value of the open area of sparging (MP5) in the smaller column.

Correlation for V_{GC}

From the foregoing discussion, it can be seen that the terminal settling velocity ($V_{SN\infty}$), volume of solids per unit cross-sectional area (ϵ'_S), column diameter, and sparger design are the controlling parameters for the critical superficial gas velocity for solid suspension (V_{GC}).

In the present work the data collected for V_{GC} was for the air–water system only. Pandit and Joshi (1987) have shown that the change in the liquid-phase physical properties exhibits a very significant effect on V_{GC}. They noted that the decrease in surface tension of liquid (by addition of alcohol) increases the V_{GC}. Addition of electrolyte also shows a similar effect. Further, an increase in the liquid viscosity (varied by the addition of glycerine) decreases the value of V_{GC}. All these effects can be explained on the basis of the fractional gas holdup (ϵ_G). It is known that in the presence of an aliphatic alcohol or an electrolyte, ϵ_G increases. In contrast, the value of ϵ_G decreases with an increase in the liquid viscosity. Therefore, the fractional gas holdup was selected as the correlating parameter in addition to the other parameters such as particle settling velocity, solid loading, and the column diameter. In correlating V_{GC} with solid loading, different authors have used different units for fractional solid loading. Roy et al. (1964) have used C'_S (kg of solid/kg of slurry), Narayanan et al. (1983) have used H_S (kg of solid/kg of liquid), and Koide et al. (1983, 1984, 1986) and Smith et al. (1987) have used C_S (kg of solid/m^3 of slurry). For a given amount of solids, an increase in H_C/T reduces C'_S, H_S, and C_S but does not affect ϵ'_S, which only depends on the column diameter. As observed in this work, an increase in H_C/T beyond a value of H_C/T of 3 does not affect V_{GC}. However the correlations of Roy et al. (1964), Narayanan et al. (1969), Koide et al. (1983, 1984, 1986), and Smith et al. (1987) will all predict different values of V_{GC} for a given amount of solids at different values of H_C/T. Hence the use of the units of fractional solid loading, C'_S, H_S, and C_S, may not be justified. Also for a given fractional solid loading in terms of C'_S, H_S, and C_S, with an increase in H_C/T, ϵ'_S increases and V_{GC} increases. Hence when a comparison is made of the effect of the column diameter on V_{GC}, if fractional solid loading units are used, different values of V_{GC} would be obtained in the two columns, depending on the value of H_C/T used in the two columns. However using ϵ'_S as a parameter, V_{GC} values could be compared in the two columns at comparable values of ϵ'_S. Hence when a correlation for V_{GC} is developed, units of fractional solid loading are not suitable, and hence ϵ'_S is incorporated in the correlation.

The following correlation was obtained for 170 data points with a standard deviation of 8%. As pointed out earlier, while this correlation was being developed, the data obtained with the single point spargers and sparger MP1 (which were inefficient) were not included. The data of Pandit and Joshi (1984, 1987) were also used, as these authors varied the physical properties of the liquids.

$$V_{GC} = 0.54 V_{SN\infty}^{0.46} \epsilon_G^{0.66} \epsilon'^{0.39}_S T^{0.27} \quad (3)$$

where

$$0.0125 < V_{SN\infty} < 0.27 \text{ m/s}$$

$$0.05 < \epsilon_G < 0.372$$

$$5.8 < \epsilon'_S < 80 \text{ mm}$$

$$0.2 < T < 0.385 \text{ m}$$

$$3 < H_C/T < 8$$

The correlation coefficient was 0.92. The above correlation holds over the entire range of $V_{SN\infty}$ and ϵ'_S covered in this work. It may be noted that the exponents on $V_{SN\infty}$ and ϵ'_S in the correlation are lower than those experimentally observed for higher values of $V_{SN\infty}$ and ϵ'_S. Further, the correlation exponents are higher for low $V_{SN\infty}$ and ϵ'_S. We could get a single correlation probably because

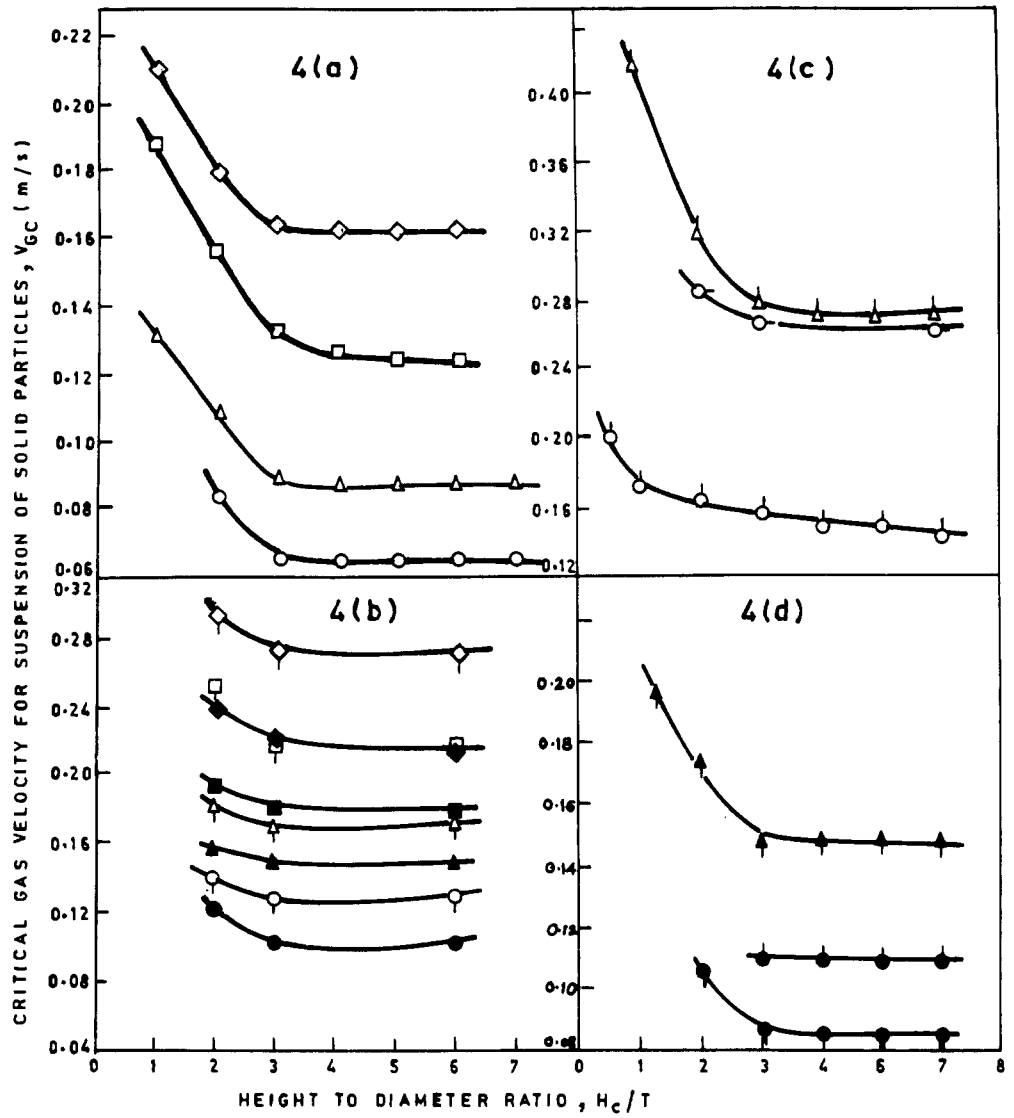

Figure 4. Effect of H_C/T on V_{GC}. (a) For sparger = MP2, d_p = 250 μm, T = 385 mm: (○) ϵ'_S = 5.8 mm; (△) ϵ'_S = 11.7 mm; (□) ϵ'_S = 17.5 mm; (◇) ϵ_S = 23.4 mm. (b) For sparger = MP2, T = 385 mm: (●) d_p = 600 μm, ϵ'_S = 5.8 mm; (▲) d_p = 600 μm, ϵ'_S = 11.7 mm; (■) d_p = 600 μm, ϵ'_S = 17.5 mm; (◆) d_p = 600 μm, ϵ'_S = 23.4 mm; (Q) d_p = 900 μm, ϵ'_S = 5.8 mm; (⏢) d_p = 900 μm, ϵ'_S = 11.7 mm; (⊡) d_p = 900 μm, ϵ'_S = 17.5 mm; (◈) d_p = 900 μm, ϵ'_S = 23.4 mm. (c) For sparger = MP2, T = 385 mm: (Ò) d_p = 1200 μm, ϵ'_S = 5.8 mm; (⏢) d_p = 1200 μm, ϵ'_S = 11.7 mm; (O-) d_p = 2100 μm, ϵ'_S = 5.8 mm. (d) For sparger MP1, T = 385 mm: (◉) d_p = 250 μm, ϵ'_S = 0.12 mm; (▲) d_p = 250 μm, ϵ'_S = 1.20 mm; (◆) d_p = 600 μm, ϵ'_S = 0.01 mm.

of the compensating effects of the two exponents. In addition, in both cases, the corresponding values of gas holdup (ϵ_G) also help in improving the correlation coefficient. It must be noted that the effect of the design of the gas sparger (hole size and number of holes) on V_{GC} has not been quantitatively incorporated in this correlation. Hence, as discussed earlier V_{GC} is lower for sparger MP4 as compared to sparger MP5, though ϵ_G with sparger MP4 is more than that with the latter sparger.

The parity plot is shown in Figure 9. It can be seen that the agreement between the predicted and experimental values is good. Also shown in this figure are the predictions of the correlations of Narayanan et al. (1969) and Koide et al. (1983). At low values of $V_{SN\infty}$ (<181 mm/s), the correlation of Narayanan et al. predicts very high values of V_{GC}, but at higher values of $V_{SN\infty}$ (>181 mm/s) the agreement between experimental and predicted values is better. At low values of solid loading, the predictions of the correlation of Koide et al. compare favorably with experimentally observed values. But at higher values of solid loading, there is a significant deviation. The correlation of Roy et al. (1964) predicts very low values of V_{GC} and hence are not shown in this figure.

For the use of eq 3, experimentally observed gas holdup values are required. However, when these are not available, empirical correlations may be used. For the estimation of gas holdup in three-phase bubble columns with air–water/pure liquids and different spargers, particle sizes, and solid loadings, the following correlation (Abraham et al., 1991) may be used:

$$\epsilon_G = 1.44[V_G^{0.71}\rho_L^{-0.18}\sigma_L^{-0.21}\{(d_o + 0.6)/d_o\}T^{-0.04}\exp\{-0.62V_{SN\infty}^{-0.47}V_G^{-0.69}\bar{\epsilon}_S\}] \quad (4)$$

Conclusions

(1) Sparger design plays an important role in deciding the suspension performance of particles in solid suspended bubble columns. The critical superficial gas velocity for solid suspension (V_{GC}) decreases with increasing number of holes. However when the number of holes is increased infinitely, V_{GC} decreases.

(2) For multipoint spargers V_{GC} decreases with an increase in H_C/T up to H_C/T = 3 but with further increase in H_C/T, there is no change in the values of V_{GC}. For single point spargers V_{GC} decreases with an increase in H_C/T up to higher values of H_C/T.

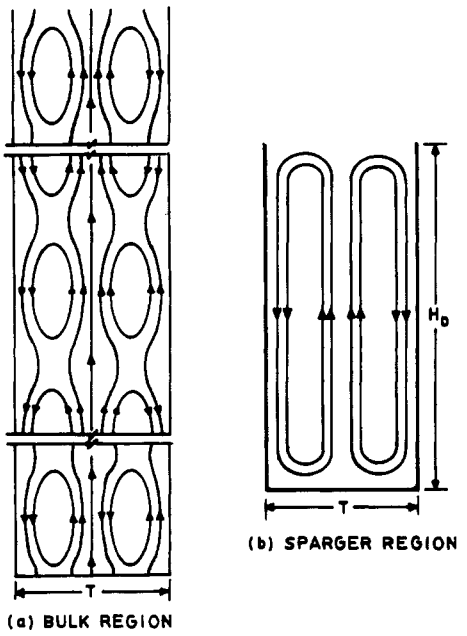

Figure 5. Flow patterns in bubble columns.

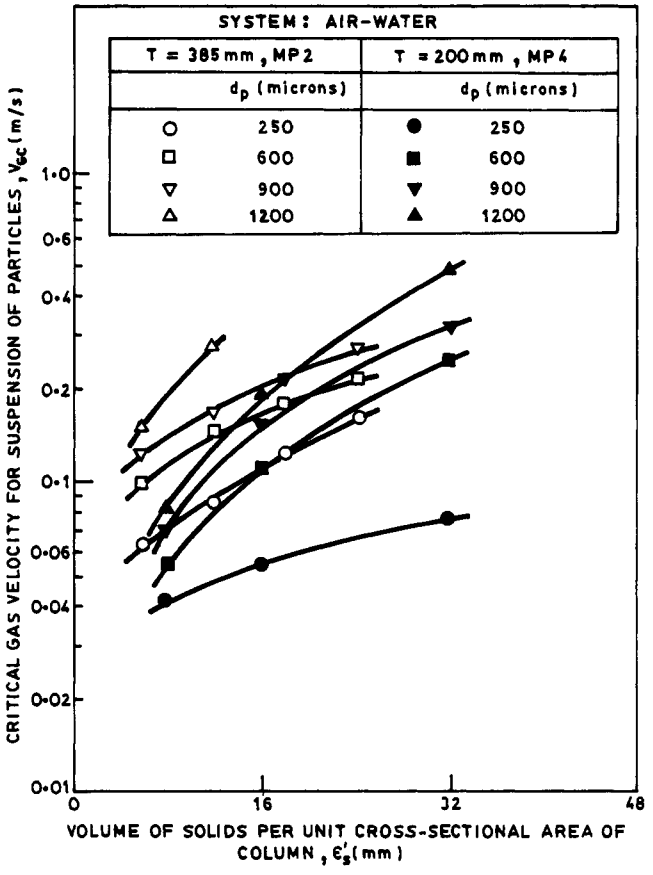

Figure 6. Effect of T on V_{GC} using spargers with comparable percent free cross-sectional areas.

(3) V_{GC} increases with increasing column diameter when spargers with similar percent free cross-sectional areas are used. V_{GC} varies as the 0.27th power of column diameter. However when spargers with widely different percent free cross-sectional areas are used in the two columns, quite different results are obtained.

(4) In the variation of V_{GC} with terminal settling velocity ($V_{SN\infty}$) and volume of solids per unit cross-sectional area of column (ϵ'_S), two distinct regimes were observed. For particles with sizes less than or equal to 600 μm (corresponding to $V_{SN\infty}$ = 100mm/s), V_{GC} varies as $V_{SN\infty}^{0.45}$ μm, and $\epsilon'^{0.25}_S$. For particles with sizes above 600 μm, V_{GC} varies as $V_{SN\infty}^{0.89}$ and $\epsilon'^{0.57-0.78}_S$.

(5) The presence of a noncoalescing agent in water increased the value of V_{GC}, whereas the presence of a coalescing agent decreased V_{GC}. The coalescing nature of

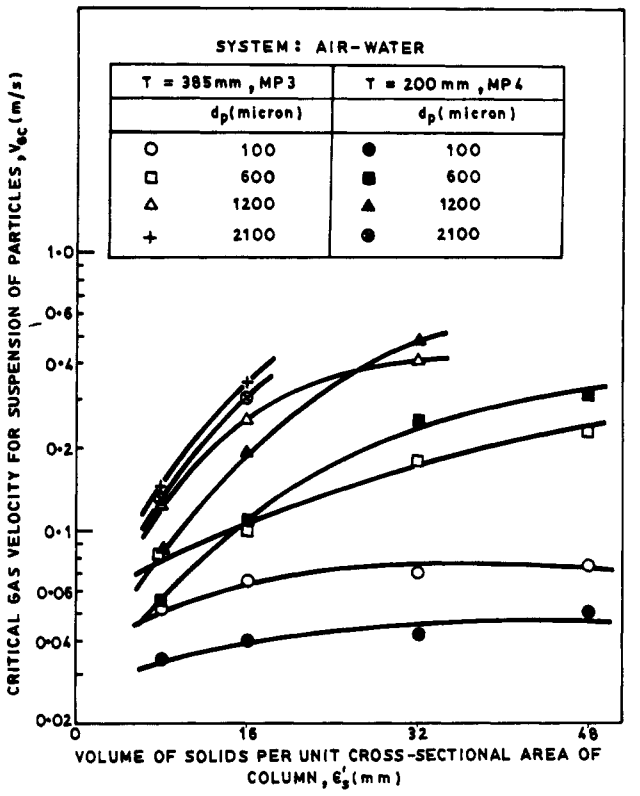

Figure 7. Effect of T on V_{GC} using spargers with widely different percent free cross-sectional areas.

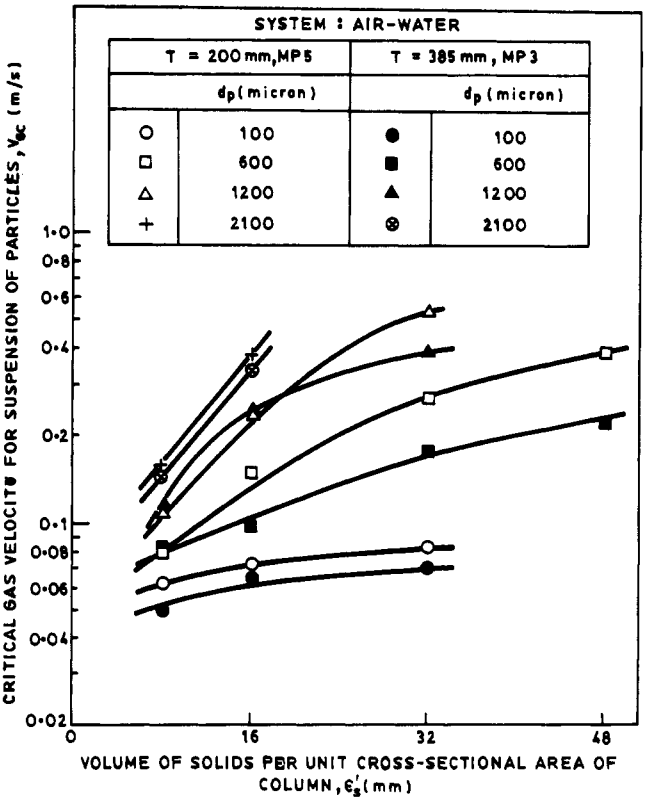

Figure 8. Effect of T on V_{GC} using spargers with widely different percent free cross-sectional areas.

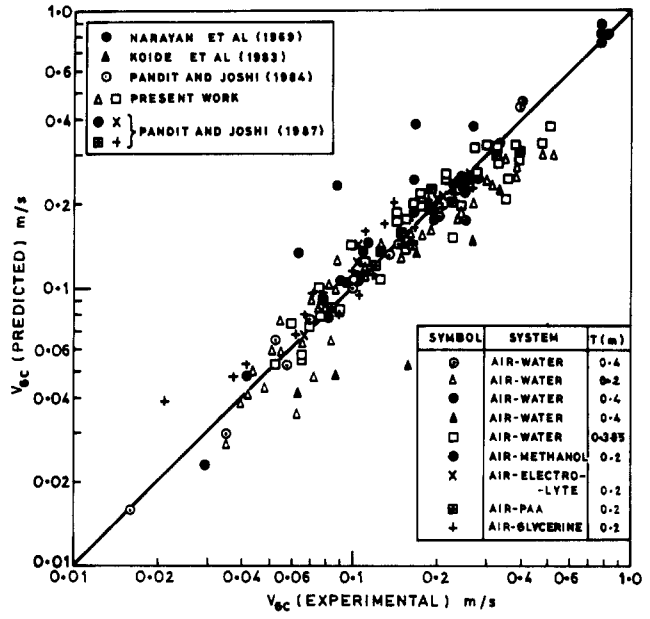

Figure 9. Parity plot for eq 3.

the liquid medium was characterized by the value of the gas holdup. In all cases it was observed that the value of V_{GC} increased with an increase in the fractional gas holdup.

The following correlation has been proposed for V_{GC}

$$V_{GC} = 0.54 V_{SN\infty}^{0.46} \epsilon_G^{0.66} \epsilon'^{0.39}_S T^{0.27} \quad (3)$$

where

$$0.0125 < V_{SN\infty} < 0.27 \text{ m/s}$$
$$0.05 < \epsilon_G < 0.372$$
$$5.8 < \epsilon'_S < 80 \text{ mm}$$
$$0.2 < T < 0.385 \text{ m}$$
$$3 < H_C/T < 8$$

Acknowledgment

M.A. thanks the University Grants Commission. A.S.K., as well as the research, was supported by a grant under the Indo–U.S. Collaborative Materials Science Programme (CE1).

Nomenclature

B = average percent solid concentration in gas free slurry (kg of solid/kg of liquid) ($=100H_s$)
C_S = average solid concentration in gas free slurry (kg of solid/m^3 of slurry)
C'_S = average solid concentration in gas free slurry (kg of solid/kg of slurry)
C_μ = viscosity correction factor
d_p = diameter of particles (m)
D_d = diameter of gas distributor (m)
d_o = diameter of orifice (mm)
D_S = longitudinal dispersion coefficient for solids (m^2/s)
g = acceleration due to gravity (m/s^2)
H = length of draft tube (m)
H_C = clear liquid height (m)
H_D = dispersed liquid height (m)
H_S = average solids concentration (kg of solid/kg of liquid)
H_{SL} = static slurry height above the bottom plate (m)
n = exponent in correlation 2, Table II
N = number of orifices
N_B = modified bubble flow number, $=\sigma/V_B\rho_L$
Re_T = superficial gas Reynolds number based on empty cross-sectional area of tube
S_a = cross-sectional area of annulus (m^2)
S_i = cross-sectional area of draft tube (m^2)
S_o = cross-sectional area of column (m^2)
T = column diameter (m)
t_w = wall thickness of draft tube (m)
U' = turbulence intensity (m/s)
V_B = average bubble rise velocity, V_G/ϵ_G (m/s)
$V_{b\infty}$ = bubble rise velocity (m/s)
V_C = liquid circulation velocity (m/s)
V_G = superficial gas velocity (m/s)
V_{GE} = experimental value of superficial gas velocity (m/s)
V_{GT} = theoretical value of superficial gas velocity (m/s)
V_{GC} = critical superficial gas velocity for suspension of solid particles (m/s)
V_L = superficial liquid velocity (m/s)
V_S = minimum pickup velocity of the fluid required to initiate the suspension of solid particles (m/s)
V_{SN} = settling velocity of nonspherical solid particles in an aerated column (m/s)
$V_{SN\infty}$ = terminal settling velocity of nonspherical particles (m/s)
V_t = stokes free settling velocity (m/s)
V_{ZB} = velocity imparted to the liquid due to movement of the bubble through the liquid column (m/s)

Greek Symbols

δ = ratio of bubble volume to wake volume
ϵ_G = fractional gas holdup
ϵ_L = average fractional liquid holdup based on clear liquid volume
$\bar{\epsilon}_S$ = average fractional solid holdup based on clear liquid volume
ϵ'_S = volume of solids per unit cross-sectional area of the column (mm)
μ = liquid viscosity (Pa·s)
ν = wettability factor
ν' = ratio of wettability of less wettable to maximum wettable solids in a particular medium
ρ_C = continuous-phase density (kg/m^3)
ρ_L = density of liquid (kg/m^3)
ρ_S = density of solid (kg/m^3)
σ = surface tension of liquid (N/m)

Literature Cited

Abraham, M.; Sawant, S. B.; Joshi, J. B. Correlations for Gas Holdup in a Three Phase Bubble Column With Water, Pure Liquids, Dilute Alcohol and Non-Newtonian Solutions. To be submitted for publication, 1991.

Doraiswamy, L. K.; Sharma, M. M. *Heterogeneous Reactions-Analysis, Examples and Reactor Design*; Wiley-Interscience: New York, 1984; Vol. 2, pp 8–12.

Heck, J.; Onken, U. Hysteresis Effects in Suspended Solid Particles in Bubble Columns with and without Draught Tube. *Chem. Eng. Sci.* **1987**, *42*, 1211–1212.

Imakufu, K.; Wang, T. Y.; Koide, K.; Kuboto, H. The Behaviour of Suspended Solid Particles in The Bubble Column. *J. Chem. Eng. Jpn.* **1968**, *1*, 153–158.

Joshi, J. B. Axial Mixing in Multiphase Contactors-A Unified Approach. *Trans. Inst. Chem. Eng.* **1980**, *58*, 155–165.

Joshi, J. B.; Sharma, M. M. A Circulation Cell Model for Bubble Columns. *Trans. Inst. Chem. Eng.* **1979**, *57*, 244–251.

Joshi, J. B.; Utgikar, V. P.; Sharma, M. M.; Juvekar, V. A. Modelling of Three Phase Sparged Reactors. *Rev. Chem. Eng.* **1985**, *3*, 281–406.

Joshi, J. B.; Shertukde, P. V.; Godbole, S. P. Modelling of Three Phase Sparged Catalytic Reactors. *Rev. Chem. Eng.* **1988**, *5*, 71–150.

Koide, K.; Yasuda, T.; Iwamoto, S.; Fukuda, E. Critical Gas Velocity Required for Complete Suspension of Solid Particles in Solid Suspended Bubble Column. *J. Chem. Eng. Jpn.* **1983**, *16*, 7–12.

Koide, K.; Horibe, K.; Kawabata, H.; Ito, S. Critical Gas Velocity Required for Complete Suspension Of Solid Particles in Solid Suspended Bubble Columns with Draft Tube. *J. Chem. Eng. Jpn.* **1984**, *17*, 368–374.

Koide, K.; Terasawa, M.; Hiroshi, T. Critical Gas Velocity Required for Complete Suspension of Multicomponent Solid Particle Mixtures in Solid Suspended Bubble Columns with and without

Draught Tube. *J. Chem. Eng. Jpn.* **1986**, *19*, 341-344.
Myauchi, T.; Shiu, C. N. Flow of Fluid in Gas Bubble Columns. *Kagaku Kogaku* **1970**, *34*, 958-965.
Narayanan, S.; Bhatia, V. K.; Guha, D. K. Suspension of Solids by Bubble Agitation. *Can. J. Chem. Eng.* **1969**, *47*, 360-364.
Pandit, A. B.; Joshi, J. B. Three Phase Sparged Reactors: Some Design Aspects. *Rev. Chem. Eng.* **1984**, *2*, 1-84.
Pandit, A. B.; Joshi, J. B. Effect of Physical Properties on The Suspension of Solid Particles in Three Phase Sparged Reactors. *Int. J. Multiphase Flow* **1987**, *13*, 415-427.
Perry, R. H.; Chilton, C. H. *Chemical Engineers Handbook*; McGraw-Hill: Singapore, 1984; pp 5.63-5.64.
Roy, N. K.; Guha, D. K.; Rao, M. N. Suspension of Solids in a Bubbling Liquid; Critical Gas Flow Rates for Complete Suspension. *Chem. Eng. Sci.* **1964**, *19*, 215-225.
Shah, Y. T. *Gas-Liquid-Solid Reactor Design*; McGraw-Hill: New York, 1979; pp 32-36.
Smith, D. N.; Ruether, J. A.; Shah, Y. T.; Badjugar, M. N. Modified Sedimentation Dispersion Model for Solids in a Three Phase Slurry Column. *AIChE J.* **1986**, *32*, 426-436.
Ueyama, K.; Myauchi, T. Properties of Recirculating Turbulent Two Phase Flow in Gas Bubble Columns. *AIChE J.* **1979**, *25*, 258-266.

Received for review May 7, 1991
Revised manuscript received October 25, 1991
Accepted November 28, 1991

Maximum Heat-Transfer Coefficient for an Immersed Body in a Bubbling Fluidized Bed

Mayumi Tsukada and Masayuki Horio*
Department of Chemical Engineering, Tokyo University of Agriculture and Technology, Koganei, Tokyo 184, Japan

The heat-transfer coefficient between the bed and an immersed body is an important parameter for determining the surface temperature of a body, which affects the rate of combustion, reaction, drying, or heat treatment. In this paper the following simple correlation for the maximum heat-transfer coefficient, $h_{s,max}$, was obtained within the accuracy of +70% and -50% by a comprehensive data set covering a wide range of operating conditions (d_p = 0.08-3 mm, d_s = 4-60 mm, temperature = 293-1323 K and pressure = 0.1-8.1 MPa): $Nu_{s,max} \equiv h_{s,max}d_s/k_e = (d_s/d_p)^{0.8}$, where d_p, d_s, and k_e are particle diameter, body diameter, and effective thermal conductivity of a bed. In this correlation, k_e was used instead of gas thermal conductivity. The correlation was successfully validated. Eleven previous correlations were tested and evaluated by the same data set.

Introduction

So far, the following knowledge has been widely accepted with respect to the gas fluidized bed heat-transfer coefficient, h_s, for "immersed bodies", i.e. small and rather spherical bodies having sizes much larger than the size of bed particles but smaller than the bed dimensions, or for other heat-transfer surfaces.

(1) The bed to surface heat-transfer coefficient increases with increasing fluidizing gas velocity. The rate of the increase jumps up at the minimum fluidization velocity, u_{mf}. Above u_{mf} a renewal of the dense phase on the surface takes place. The renewal rate controls the heat-transfer rate. Below u_{mf}, there is no renewal of the dense phase and the heat-transfer rate is controlled mainly by the resistance between surface and interstitial gas.

(2) If the gas velocity is increased continuously, h_s reaches a maximum, $h_{s,max}$, and then starts decreasing gradually. This decrease is because of the increased occupation of the surface area by the bubble phase.

(3) The above two features appear less obvious for coarse particle beds, where the surface to interstitial gas heat transfer is more significant than it is in the case of fine particle beds.

For the past two decades, fluidized bed to surface heat transfer has been investigated intensively with the focus being on fluidized bed combustor developments. Since the combustion efficiency of bubbling fluidized bed boilers is determined by the balance of the combustion rate and elutriation rate of char particles, the surface temperature of burning char is quite important. The surface temperature also affects NO_x decomposition on the char surface. In this regard the heat transfer between the fluidized bed and immersed or floating bodies is quite significant. It is also related to fluidized bed drying and heat treatment.

The heat-transfer characteritics of bed to immersed bodies would be a bit different from those of bed to heat exchange surface because (1) immersed bodies are rather spherical in shape; (2) the diameters of immersed bodies in industrial processes range quite widely from 10^{-3} to 0.1 m and often change with time; (3) in most cases immersed bodies move within the bed; and (4) surface temperatures of bodies relevant to industrial processes vary widely, depending on heat of surface reactions if they exist.

With respect to the bed to immersed body heat-transfer coefficient, Ross et al. (*1*) determined a bed to burning char heat-transfer coefficient from combustion experiments. They also assumed fluidized particles as a continuum. On the same line, Prins et al. (*2*) tried to develop a Ranz-Marshall type correlation for h_s. The correlation introduced a new difficulty since it required the knowledge of the bed effective viscosity.

In our previous work (*3*), the bed to sphere heat-transfer coefficient was measured over wide experimental conditions (immersed body diameter d_s = 6.35-19.05 mm, particle diameter d_p = 0.14-0.55 mm, bed temperature T_b = 293-1123 K), and the following simple empirical correlation was obtained:

$$Nu_{s,max} \equiv h_{s,max}d_s/k_e = 10d_s^{0.8}d_p^{-0.5} \quad (\pm 20\%) \quad (1)$$

In this correlation the effect of radiation was successfully included in the bed effective thermal conductivity k_e. The objective of the present work is to obtain a more widely applicable but simpler correlation for the bed to immersed body maximum heat-transfer coefficient through comprehensive evaluation of previous data and correlations.

Previous Works

There are quite a few review on fluidized bed heat transfer (*4-15*), but not much information is available concerning bed to immersed body heat transfer. In this section previous works are reviewed, with a focus on this particular aspect.

0888-5885/92/2631-1147$03.00/0